# Role of Distal Arginine in Early Sensing Intermediates in the Heme Domain of the Oxygen Sensor FixL†

Audrius Jasaitis,‡ Klara Hola,‡,§ Latifa Bouzhir-Sima,‡ Jean-Christophe Lambry,‡ Veronique Balland,|| Marten H. Vos,*,‡ and Ursula Liebl‡

*CNRS, UMR 7645, Laboratory for Optical Biosciences, Ecole Polytechnique, 91128 Palaiseau Cedex, France, INSERM, U696, 91128 Palaiseau Cedex, France, Institute of Microbiology, Academy of Sciences of the Czech Republic, Videnska 1083, 142 20 Prague 4, Czech Republic, and Laboratoire de Biophysique du Stress Oxidant, SBE/DBJC and CNRS URA 2096, CEA/Saclay, 91191 Gif-sur-Yvette cedex, France*

*Received January 4, 2006; Revised Manuscript Received March 24, 2006*

ABSTRACT: FixL is a bacterial heme-based oxygen sensor, in which release of oxygen from the sensing PAS domain leads to activation of an associated kinase domain. Static structural studies have suggested an important role of the conserved residue arginine 220 in signal transmission at the level of the heme domain. To assess the role of this residue in the dynamics and properties of the initial intermediates in ligand release, we have investigated the effects of R220X (X = I, Q, E, H, or A) mutations in the FixLH heme domain on the dynamics and spectral properties of the heme upon photolysis of $O_2$, NO, and CO using femtosecond transient absorption spectroscopy. Comparison of transient spectra for CO and NO dissociation with steady-state spectra indicated less strain on the heme in the ligand dissociation species for all mutants compared to the wild type (WT). For CO and NO, the kinetics were similar to those of the wild type, with the exception of (1) a relatively low yield of picosecond NO rebinding to R220A, presumably related to the increase in the free volume of the heme pocket, and (2) substantial pH-dependent picosecond to nanosecond rebinding of CO to R220H, related to formation of a hydrogen bond between CO and histidine 220. Upon excitation of the complex bound with the physiological sensor ligand $O_2$, a 5−8 ps decay phase and a nondecaying (>4 ns) phase were observed for WT and all mutants. The strong distortion of the spectrum associated with the decay phase in WT is substantially diminished in all mutant proteins, indicating an R220-induced role of the heme in the primary intermediate in signal transmission. Furthermore, the yield of dissociated oxygen after this phase (∼10% in WT) is increased in all mutants, up to almost unity in R220A, indicating a key role of R220 in caging the oxygen near the heme through hydrogen bonding. Molecular dynamics simulations corroborate these findings and suggest motions of $O_2$ and arginine 220 away from the heme pocket as a second step in the signal pathway on the 50 ps time scale.

In the bacterium *Bradyrhizobium japonicum* (*Bj*),[1] the FixL/FixJ two-component regulatory system is part of the signaling cascade that enables the organism to adapt its respiratory metabolism to the aerobic or microaerobic state of its environment. FixL is a heme-containing multidomain protein (*1*). It contains a histidine kinase domain that phosphorylates the transcription factor FixJ and an oxygen-sensing heme domain FixLH (*2*, *3*). The kinase activity of this protein dramatically decreases when oxygen binds to the heme. FixL activity is also modulated by binding of other gaseous ligands such as CO and NO, but to a far lesser extent (*4*).

FixLH belongs to the family of PAS domains which possess a conserved fold binding various cofactors and are frequently involved in transducing structural protein changes, in the case of FixL in response to the binding of diatomic molecules. Several X-ray crystallographic structures of the *Bj*FixL heme domain in the ferric and ferrous unliganded state and with various ligands bound to the heme are available (*5*−*8*) as well as the three-dimensional structure of FixLH from *Rhizobium meliloti* (*9*). These structures provide models for the starting and end points of signal transmission within the heme domain, and mechanistic models for the pathway between these points have been proposed (*6*, *9*).

Elements of the transmission pathway can in principle be experimentally unravelled using time-resolved studies, initiated by ligand binding or dissociation. In particular, the fact that in FixL the signaling molecule binds to a heme cofactor can be exploited, as diatomic ligands can be photodissociated using a short light pulse, allowing subsequent observation of very short-lived intermediates in the liganded → unliganded pathway. The kinetics of ligand binding and the

† A.J. was the recipient of an EMBO long-term fellowship, and K.H. was the recipient of an EC Marie Curie Training Site fellowship.

* To whom correspondence should be addressed. Telephone: +33169084777. Fax: +33169083017. E-mail: marten.vos@polytechnique.edu.

‡ CNRS UMR 7645 and INSERM U696.

§ Academy of Sciences of the Czech Republic.

|| CEA/Saclay.

[1] Abbreviations: *Bj*, *Bradyrhizobium japonicum*; FixLH, heme domain of FixL; MD, molecular dynamics; WT, wild type.

10.1021/bi060012i CCC: $33.50 
Published on Web 04/18/2006

spectral characteristics of intermediates have been studied using various spectroscopic techniques (*10*−*13*). As in most heme proteins, CO rebinding is essentially bimolecular and can be studied with nanosecond and lower time resolution. In this way, resonance Raman spectroscopy with nanosecond pulses provided indications that the heme structure of the CO-photodissociated complex differs from the relaxed deoxy state (*11*), and transient absorption data suggested that on a millisecond time scale the relaxed deoxy state is recovered (*13*). In view of the high yield of geminate heme−ligand rebinding (*12*), the characterization of the dissociated complex for NO and the physiological ligand $O_2$ requires a much higher time resolution. Using femtosecond transient absorption spectroscopy, we have previously shown substantial constraints on the heme spectrum upon excitation of the liganded FixLH complexes in the order $O_2$ > NO > CO (*12*), implying the buildup of intermediate states between heme-liganded and relaxed unliganded states. In addition, specifically for oxygen, extremely fast (5 ps) re-formation of the steady-state heme−$O_2$ complex was observed with only ∼10% $O_2$ escaping from the heme pocket (*12*). Thus, despite the low oxygen affinity (130 $\mu$M) (*10*), the heme pocket efficiently traps oxygen and acts as a picosecond "bistable switch", which allows a fraction of dissociated oxygen to bring about the ensemble of further intermediates in the sensing process. Although the steady-state heme configurations are very similar to those in nonsensor heme proteins such as myoglobin, the spectral characteristics of the transients are dramatically different, implying a specific role of the protein environment in the transiently formed initial signaling intermediate.

A conserved arginine residue (R220 in *B. japonicum*) is present in all known FixL proteins, and its equivalent is also found in the distal pocket of the related *Ec*Dos heme-based sensor protein (*14*). This residue has been proposed to play a crucial role in ligand discrimination and in the signal transmission pathway, because of its striking rearrangement between the oxy complex, where R220 is hydrogen-bonded to the terminal oxygen atom, and the deoxy-, NO-, and CO-bound states, where it interacts with propionate 7 of the heme (*6*, *7*). Indeed, a characterization of the R220A mutant of *Bj*FixL revealed modifications of the heme structure and oxygen affinity as well as changes the activity of the enzymatic domain and its regulation (*15*).

To further probe the role of R220 in ligand sensing and early signaling, we have constructed several position 220 mutants of FixLH. Mutations of R220 to I, Q, H, and E were selected to alter the electrostatic and hydrogen bonding properties, with minor steric modifications, and the mutants were characterized by their steady-state resonance Raman spectra and bimolecular ligand interaction properties (*16*, *17*). In addition, the FixLH R220A mutant in which steric modifications are quite substantial was constructed (*15*). For all mutant proteins, the ligand binding and dissociation rates were found to be substantially increased and the overall oxygen affinity was found to be modified (*16*). In this work, we study the influence of these mutations on the initial dynamics and heme perturbations after ligand dissociation using femtosecond spectroscopy. Along with molecular dynamics simulations, our results imply that the presence of the conserved arginine residue at position 220 strongly, but not exclusively, determines the strain on the heme in the initially formed transmission intermediate and the "oxygen cage" properties of the heme pocket.

## MATERIALS AND METHODS

*DNA manipulations, protein expression, and purification* were performed as previously described (*16*).

*Sample Preparation.* FixLH was prepared to a heme concentration of 50−70 $\mu$M in a gastight optical cell with an optical path length of 1 mm. Unless specified otherwise, the buffer was 50 mM Hepes buffer (pH 8.0). For the deoxy form of the protein, the degassed as-prepared (ferric) sample was reduced with 10 mM sodium dithionite. For the CO form, the deoxy form was equilibrated with 1 atm (1 atm = 101.3 kPa) of CO. For measurements in the presence of $O_2$ and NO, the degassed sample in the ferric state was reduced with 10 mM ascorbate, using 10 $\mu$M hexamine ruthenium as a mediator, and subsequently equilibrated with 1 atm of $O_2$ and 0.01 atm of NO, respectively.

*Spectroscopy.* Steady-state spectra were recorded using a Shimadzu UV−vis 1601 spectrophotometer. Multicolor femtosecond absorption spectroscopy (*18*) was performed with a 30 fs pump pulse centered at 565 nm and a <30 fs white light continuum probe pulse, at a repetition rate of 30 Hz. Full spectra of the test and reference beams were recorded using a combination of a polychromator and a CCD camera. Multiple time window acquisition schemes were used, with windows ranging from 4 ps to 4 ns full scale. All experiments were carried out at 21 °C. The sample was continuously moved perpendicular to the beams to ensure sample renewal between subsequent pulse pairs.

Basic data matrix manipulations and presentation were performed using Matlab (The Mathworks, South Natick, MA). The absorbance changes were globally analyzed in terms of a multiexponential model and decay-associated spectra using the SPLYMOD algorithm (*19*), with a Matlab interface (*20*).

*Molecular Dynamics Simulations.* A model of the oxy complex of the *B. japonicum* FixLH heme domain was constructed using the molecular modeling program CHARMM (*21*) (version 30b1) and the crystal structure of the wild type *Bj*FixLH oxy complex (Protein Data Bank entry 1DP6) (*6*). The model includes 104 residues (154−257), one heme, one dioxygen ligand, and 1031 water molecules that surround the protein.

Simulations were performed with a relative dielectric constant of 1 for the entire structure and with a time integration step of 1 fs. Hydrogen atoms were generated using the "HBUILD" CHARMM command. The length of bonds with hydrogen atoms was fixed using the SHAKE algorithm, and nonbonded interactions were gradually set to zero between 8 and 14 Å. After energy minimization using SD and ABNR algorithms, a heating phase from 0 to 300 K over 30 ps and an equilibration phase at 300 K over 300 ps were performed. Free dynamic simulations over 500 ps for WT and 200 ps for mutants with restart backup each 50 ps were achieved. The backbone root-mean-square deviation between the crystal structure and the simulated structure remains below 1.2 Å at all times before dissociation.

Oxy complex models for mutants in which position 220 was occupied by I or A were generated starting from the WT X-ray structure using the same procedure, after deletion

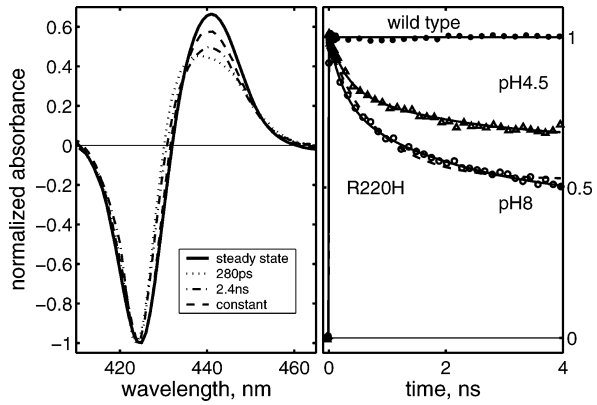


FIGURE 1: CO recombination in the R220H mutant of FixLH. In the right panel is a comparison of kinetics at 442 nm in the wild type (●) and the R220H mutant at pH 8.0 (○) and 4.5 (▲, in 50 mM acetate buffer). The dashed line through the R220H pH 8.0 data is a fit to a single exponential and a constant. The solid lines through the data at both pHs are fits to two exponentials (280 ps and 2.4 ns) and a constant. In the left panel are normalized spectra of components from the multiexponential fit: 280 ps phase (···), 2.4 ns phase (•−•), nonrelaxing phase (- - -), and steady-state CO binding difference spectrum (—). The spectra are normalized at 425 nm; the relative amplitude of the phases is 0.25 (280 ps), 0.35 (2.4 ns), and 0.40 (constant).

of the lateral chain atoms at position 220 and construction of the new atoms with the "IC BUILD" CHARMM command. For WT, R220 was constrained during the equilibration phase to prevent it from "swinging out" of the heme pocket. During the free dynamics of the oxygen-bound form, where the constraint was released, this residue remained in the heme pocket.

Ligand dissociation was simulated by deletion of the bond between heme iron and the dioxygen ligand from the bond list and simultaneous switching of heme parameters from six-coordinate to five-coordinate. The small quadrupolar charge distribution of dioxygen was simulated using a three-charge model (*22*). Different starting conditions of the model before ligand dissociation were obtained by prolonging the free dynamic phase of the oxygen-bound form by subsequent periods of 50 ps. Atom coordinates of the simulated structures were saved each picosecond for further analysis.

## RESULTS

*CO Dissociation and Rebinding.* The steady-state spectra of the FixLH−CO complexes of the different mutant proteins are all similar to those of WT (*16*). As in WT FixLH, with the R220A, R220E, R220Q, and R220I substitutions, the transient spectra were unchanged on the time scale of 4 ps to 4 ns and rebinding of CO to the heme was not observed on this time scale. In WT, the transient spectrum is somewhat altered compared to the steady-state difference spectrum (*12*). In the four above-mentioned mutants, this spectral perturbation was considerably smaller.

In the R220H mutant protein, the CO dynamics are strikingly different. Here substantial heme−CO rebinding does occur in the first few nanoseconds (Figure 1). The rebinding kinetics are described by at least two rebinding phases. A best fit was obtained with time constants of 280 ± 50 ps (25% of the recovery of the bleaching) and 2.4 ± 0.8 ns (35%), and a constant (40%) (the quality of a fit with two exponentials and no constant was slightly, but significantly, lower as judged from the residuals), implying that at most ∼40% of the dissociated CO escapes from the protein. The spectra associated with the decay phases and the asymptotic phase deviate from the steady-state difference spectrum, implying an intermediate heme configuration. This is the case in particular for the spectrum of the faster, 280 ps phase, which is more perturbed than the spectrum associated with dissociated CO in WT FixLH on a similar time scale (*12*), suggesting that the relatively rapid heme−CO rebinding is at least partially due to a constrained heme configuration associated with the presence of a distal histidine.

Table 1: NO Recombination Properties in WT and Different Mutants of FixLH

| | fast phase | | middle phase | | slow phase | | |
|---|---|---|---|---|---|---|---|
| | $\tau$ (ps) | Amp (%) | $\tau$ (ps) | Amp (%) | $\tau$ (ps) | Amp (%) | constant (%) |
| wild type | 4.6 | 70 | 17 | 20 | 190 | 5 | 5 |
| R220H | 8.5 | 83 | 25 | 10 | 1100 | 4 | 3 |
| R220Q | 8.7 | 62 | − | − | 190 | 28 | 10 |
| R220A | 8.5 | 50 | − | − | 105 | 17 | 33 |

When the pH was lowered from 8.0 to 4.5, the relative amplitude of both decay phases decreased (Figure 1). This observation correlates well with a change in the distribution of CO interactions in the CO complex of the R220H as inferred from Fourier transform infrared spectroscopy (see the Supporting Information). These observations reflect conformational changes in the CO environment presumably related to the protonation state of H220 (see Discussion).

*NO Dissociation and Rebinding.* To study the interaction of FixLH with oxygen and nitric oxide, the degassed sample was reduced with ascorbate (see Materials and Methods). In all mutants, the reduction of the sample was complete, with the exception of R220E [which has a relatively low redox potential (*17*)], where it amounted to only ∼40%.

In the mutants, a stable complex with NO was obtained only for R220H, R220Q, and R220A. The NO rebinding properties of the mutants and wild type are summarized in Table 1. All kinetics are multiphasic, as generally observed in heme proteins (*23*), and are qualitatively similar. In wild-type FixLH, the decay kinetics can be fit with three exponential phases on the picosecond time scale (Figure 2) with similar spectral features. Five percent of NO does not rebind on this time scale, and no further decay was observed up to 4 ns (not shown); therefore, it may escape to the medium (*12*).

The overall rebinding kinetics are somewhat slower for all mutant proteins. The amplitude of the asymptotic phase is similar to that of WT for the R220H and R220Q mutant proteins. A significant influence of the mutation on the release of NO was observed in the R220A mutant, where roughly 33% of NO may escape from the heme pocket (Figure 2).

The transient spectra were different from the steady-state difference spectra, in that the induced absorption lobes were relatively weak, but for all mutants, this perturbation was far less pronounced than for WT. As for the qualitatively similar observation for CO (see above), this implies that in the mutants the ligand-dissociated heme adopts a configuration which is closer to the steady-state unliganded heme than in WT.

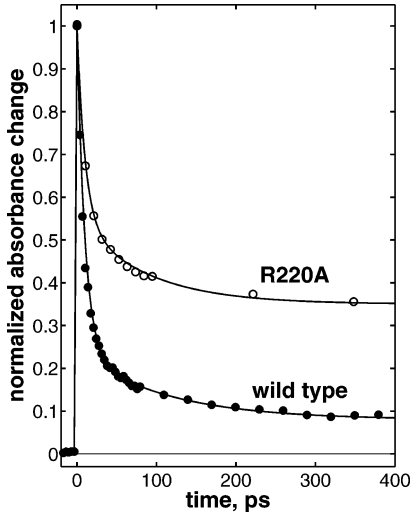


FIGURE 2: NO recombination kinetics in wild-type FixLH and the R220A mutant in the bleaching part of the spectrum (420 nm). Data are normalized.

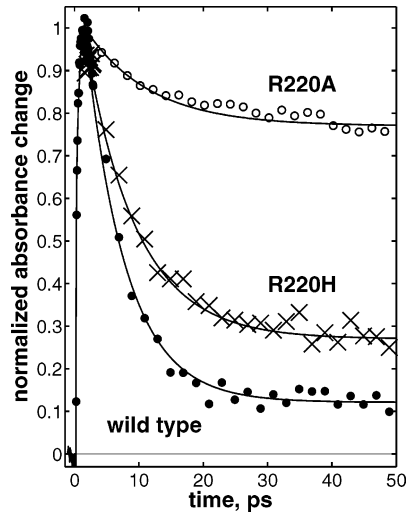


FIGURE 3: Kinetics at 442 nm of oxygenated FixLH: wild type (●), R220A (○), and R220H (×). Lines represent the global exponential fits of the data.

*$O_2$ Dissociation and Rebinding.* In the wild-type FixL heme domain, excitation of the oxy complex leads to a state characterized by a spectrum that is strongly perturbed in the induced absorbance part compared to the steady-state oxygen binding. This state decays extremely fast, in a single-exponential process with a time constant of ∼5 ps (Figures 3 and 4A), which we previously assigned to highly efficient geminate recombination of oxygen and heme (*12*). Only ∼10% of photolyzed oxygen leaves the heme pocket and can escape to the bulk.

In most mutant proteins, the oxygen binding properties were altered compared to those of the wild-type form, in which ∼98% of the FixLH population is oxygen-bound (Table 2) upon exposure to 1 atm of $O_2$. Under these conditions, the R220H mutant fully binds oxygen and the R220Q mutant ∼80% (*16*). Upon addition of $O_2$ to the R220A, R220E, and R220I mutants, a mixture of ferric, oxy, and deoxy states was obtained (Table 2). The steady-state oxygen binding properties differed most in the R220A mutant, where after addition of 1 atm of oxygen 70% of the sample was found to be oxidized, 10% remained in the deoxy

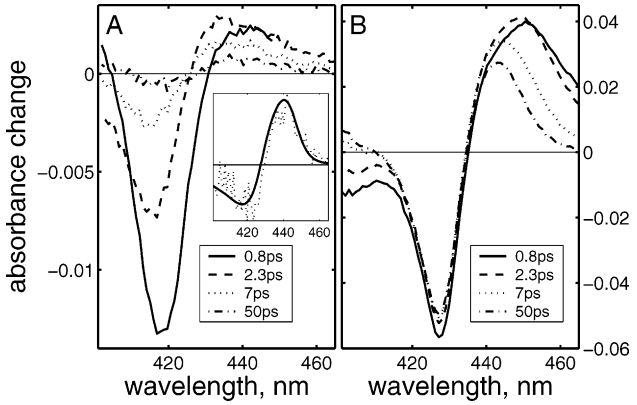


FIGURE 4: Difference spectra at selected time delays after excitation of oxygenated WT (A) and R220A (B) FixLH. The inset in panel A compares the spectrum of the long-lived (>4 ns) phase of WT FixLH (···) with the steady-state deoxy-minus-oxy difference spectrum (—).

Table 2: Reduction and Oxygen Recombination Properties in Different Mutants of FixLH

| | reduction (%) | $O_2$ binding (at 1 atm of $O_2$) deoxy (%) | oxy (%) | ferric (%) | $\tau$ of the oxygen rebinding phase (ps) | constant phase (%) |
|---|---|---|---|---|---|---|
| wild type | 100 | 2 | 98 | − | 5.1 | 10 |
| R220Q | 100 | 20 | 80 | − | 8.3 | 65 |
| R220H | 100 | − | 100 | − | 7.1 (50%), 600 (30%) | 20 |
| R220A | 100 | 10 | 20 | 70 | 5.2 | 95 |
| R220I | 100 | 40 | 50 | 10 | 5.2 | 90 |
| R220E | 40 | 20 | 20 | 60 | 4.9 | 80 |

state, and only 20% bound oxygen. Comparison of these values with those reported for the full-length R220A protein (*15*) indicates a slightly higher autoxidation rate and oxygen affinity for $O_2$ of the isolated heme domain.

The steady-state oxygen binding properties complicate the assessment of the light-induced spectral dynamics associated specifically with the oxy complexes, as the excited-state decay of the deoxy and ferric complexes also gives rise to transient signals in the first few picoseconds (*12*, *24*). However, the ferric and deoxy complexes can be easily prepared in pure form, and the transient spectral features (which are relatively weak for the case of ferric hemes) can be measured under the same experimental conditions. As in the wild type (*12*), the ground state of both ferric and deoxy mutant species was recovered with a decay component of ∼5 ps (not shown). The spectral evolution associated with these decay components can be taken into account in the analysis of the oxygenated samples as described below.

For the R220H mutant, where 100% oxy complex is formed, our analysis shows two decay processes with distinct spectra on the time scale of a few picoseconds. The spectrum of the fastest phase (∼5 ps) is significantly red-shifted with respect to the steady-state oxygen dissociation spectrum (Figure 6) and can be ascribed to the decay of an excited state, as in other heme proteins (*25*). A second decay phase (∼7 ps) has a spectrum very similar to the steady-state difference spectrum and can be assigned to geminate oxygen recombination. The amplitude of this phase amounts to roughly half of the dissociated oxygen (due to the closeness of the two time constants, this value should be considered a rough estimate). Finally, 50% of the remaining dissociated

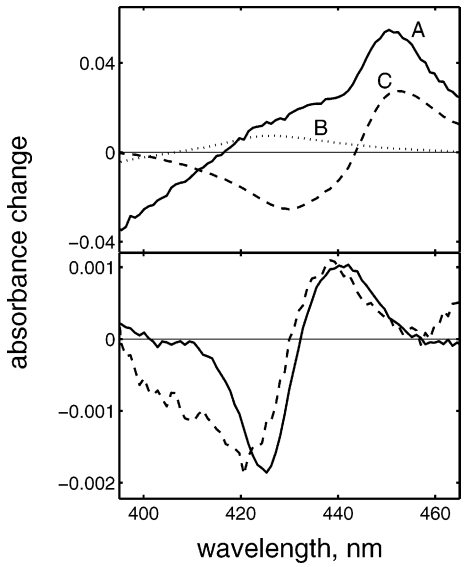


FIGURE 5: Analysis of spectral components associated with oxygen recombination in the R220E mutant of FixLH. In the top panel are spectra associated with the 5 ps component of the oxygenated complex (A, —), the ferric complex (B, ···), and the deoxy complex (C, - - -), obtained under the same concentration and excitation conditions. In the bottom panel (A − 0.6 × B − 0.2 × C) are the reconstructed spectrum associated with the 5 ps component of the oxy complex (- - -) and the constant component divided by 5 (—).

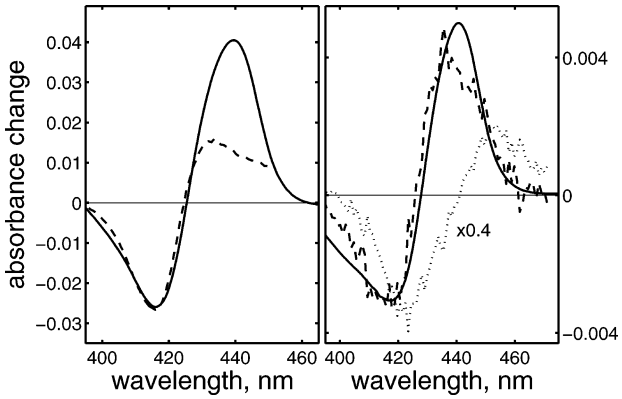


FIGURE 6: Decay components associated with excitation of wild-type FixLH and R220H oxy complexes. In the left panel is a comparison of the steady-state oxygen binding spectrum (—) and the 4.7 ps decay component (- - -) in WT. In the right panel is the same comparison in R220H: steady-state spectrum (—), 5 ps component (···), and 8 ps component (- - -).

$O_2$ recombines in ~600 ps (not shown) and the remainder in >4 ns. $O_2$ rebinding on the time scale of 10 ps to 4 ns is not observed in any of the other mutants or in WT.

For the R220Q substitution, sub-10 ps decay components with time constants similar to those for R220H were found (not shown) with the 5 ps component showing a somewhat different shape due to the contribution of a fraction of the excited deoxy complex. For this mutant protein, the fraction of geminate rebinding (in ~8 ps) was ~35%.

For the R220A, R220E, and R220I substitutions, a single picosecond decay component with a time constant of ~5 ps and a constant phase were sufficient to describe the data (Table 2). In principle, the 5 ps component contains contributions from photophysics of the deoxy and ferric forms, as well as from heme−oxygen recombination and/or photophysics of the oxy complex. After subtraction of the deoxy and ferric contributions, for all three mutants a weak

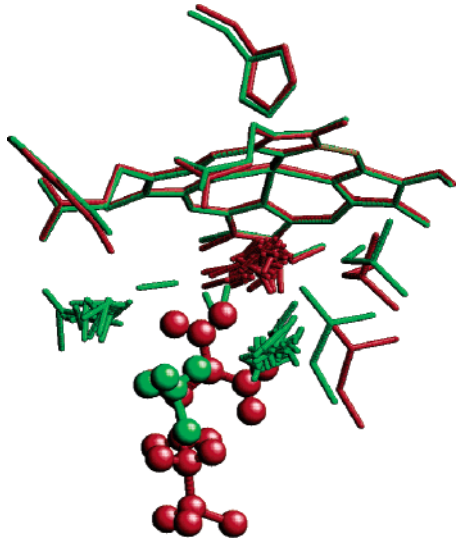

FIGURE 7: Molecular dynamics simulations. Comparison of dynamics upon oxygen dissociation in two typical 50 ps trajectories of WT (red) and R220A (green) FixLH. The position of dissociated oxygen (sticks) at 1 ps intervals is overlaid with one structure of the heme and selected residues (R220 and A220 as balls and sticks). This figure was prepared by using RASMOL (*32*).

spectrum was found that was roughly similar to the steady-state oxygen dissociation spectrum of WT and the R220H and R220Q mutants.[2] Figure 5 illustrates this for the case of the R220E substitution. For all three mutant proteins, the amplitude of this phase was less than 20% of that of the remaining constant phase (Table 2 and Figure 5), which was also similar to the steady-state difference spectrum.

The ensemble of these analyses shows that for all mutant proteins geminate rebinding of oxygen and heme occurs on a time scale of 5−10 ps but that the spectrum associated with this phase is much more similar to the steady-state deoxy-minus-oxy spectrum than in WT. The relative amplitude of the constant phase (time constant of >4 ns) is variable, but in all mutants, it is much higher than in WT.

*Molecular Dynamics Simulations.* To gain insight into the molecular factors determining the fate of oxygen in the heme pocket, we performed molecular dynamics simulations of wild-type and mutant FixLH. In these studies, after equilibration of the oxygen-bound complex, the Fe−$O_2$ bond is suddenly discarded and trajectories of the system are continued for a time window of 50 ps. This procedure is repeated for several independent initial conditions at the bond-breaking instant. In these classical simulations, after dissociation, possible bond reformation is not taken into account. In WT FixLH, after deletion of the heme iron−oxygen bond, in most simulations the oxygen molecule does not move away but fluctuates in the vicinity of its initial position close to the heme iron (red structure in Figure 7). In all trajectories of the mutants, oxygen exhibits a higher mobility and moves farther from the heme in the 50 ps time span. In the R220I mutant, oxygen always follows a trajectory out of the heme pocket via isoleucine 215, valine 222, and isoleucine 220. In the R220A mutant (Figure 7), within a few picoseconds, the ligand diffuses via either a

[2] A steady-state deoxy-minus-oxy spectrum cannot be directly obtained for the R220A, R220E, and R220I mutants due to the substantial amount of ferric heme-containing protein contributing to the oxygenated samples.

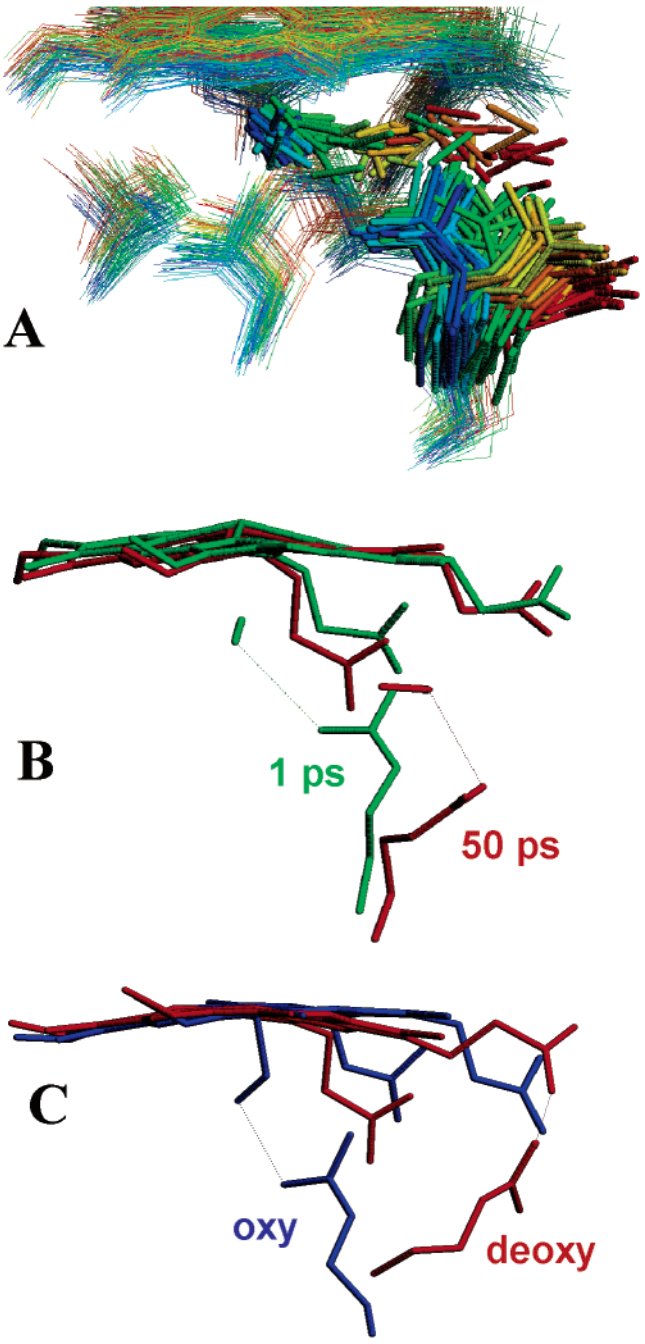


FIGURE 8: Molecular dynamics of WT FixLH during one of the few simulation trajectories in which oxygen leaves the heme pocket (see the text). (A) Superposition of structures at 1 ps intervals between −50 and 50 ps with respect to Fe−$O_2$ dissociation. Blue to red color coding refers to increasing time. (B) Structures of heme, $O_2$, and R220 1 ps (green) and 50 ps (red) after dissociation. (C) Crystal structures of the oxy complex (blue) and the deoxy complex (red), taken from Protein Data Bank entries 1DP6 (*6*) and 1LSW (*7*), respectively. In panels B and C, dashed lines represent selected hydrogen bonds and salt bridges inferred from the structures and from the simulations. This figure was prepared using RASMOL (*32*).

pathway leading to a cleft inside the protein delimited by isoleucine 215, leucine 236, and isoleucine 238 (distance to the heme iron of ~7.5 Å) or a pathway similar to that of the R220I mutant.

For WT FixLH, in five of the 13 dissociation simulations, oxygen does move out of the heme pocket. Strikingly, this motion can be associated with a conformational change of arginine 220. In two cases, the R220 side chain follows the oxygen molecule and the interaction energy between oxygen and the arginine side chain is consistent with the hydrogen bond remaining intact during and after this long-distance motion (right panel of Figure 7). In these cases, R220 moves toward its configuration in the deoxy state of FixLH (Figure 8B). However, in all cases, on the 50 ps time scale, heme propionate 7 remains in close interaction with R206 and does not adopt a conformation in which a salt bridge with R220 can be established, as observed in the deoxy structure (Figure 8C). In three of the five trajectories, R220 remained in the heme pocket while $O_2$ moved out. The inverse was not observed, suggesting that the R220 sweep in the direction of the propionates requires $O_2$ to be absent from the heme pocket.

## DISCUSSION

This work concerns the influence of the distal arginine 220 on the interaction between diatomic ligands and the heme in the FixL heme sensor domain. Our findings demonstrate that the presence of an arginine residue at position 220 is largely responsible for (a) the perturbations of the ligand-dissociated five-coordinate (5-c) heme compared to the steady-state deoxy heme (5-c without ligand in the heme pocket) and (b) the strong reactivity of the heme toward the dissociated physiological sensor ligand $O_2$. These results are corroborated by molecular dynamics simulations that indicate a continued interaction between heme-released oxygen and heme via the hydrogen bond with R220 in WT.

*Spectral Perturbations of 5-c Heme.* In WT FixL, dissociation of the heme-bound ligand can be seen as the first step in the transmission of the signal toward the enzymatic domain. The subsequent steps involve additional modification of the heme electronic configuration, as the absorption spectrum of the ligand-dissociated heme is modified with respect to the steady-state 5-c heme (the final configuration in the signaling process), especially for $O_2$ as the ligand (*12*). Several studies have indicated that R220 is one of the key residues involved in the transmission process (*5*, *6*, *15*, *16*). In this work, we show for substitutions of arginine at position 220, that the spectral perturbations are strongly diminished compared to the WT FixLH spectrum and that the heme adopts a "deoxy-like" configuration within a few picoseconds of ligand dissociation. This implies that R220 is strongly involved in the postdissociation transmission steps involving the heme.

In the WT FixLH−$O_2$ complex, R220 forms a hydrogen bond with the terminal oxygen atom of heme-bound $O_2$ (*6*). As isoleucine and alanine are incapable of hydrogen bonding, the decrease in the extent of heme perturbation seen in the dissociated $O_2$ complexes of the R220I and R220A mutants might be ascribed to this fact. However, similar effects on the transient spectra of the dissociated oxy complexes were observed with other substituted residues that are capable of H-bonding (glutamine and histidine). Indeed, Raman data indicate H-bonding of the terminal oxygen atom in the R220H FixLH−$O_2$ complex (*16*). Furthermore, hydrogen bonding of heme-bound ligands with a distal histidine residue occurs in other nonsensor, heme proteins such as myoglobin, without sizable spectral effects on the picosecond transient spectra. Together, we can ascribe the strongly perturbed

transient spectra in WT FixLH largely to the specific influence of arginine 220. Our previous steady-state resonance Raman characterization of the FixLH−$O_2$ complex indicates a strong H-bond between R220 and the terminal oxygen atom as well as an unusual influence on the heme, possibly resulting in a slight doming of the heme iron toward the $O_2$ ligand (*16*). This feature and the proximity of $O_2$ after dissociation, as suggested from our MD simulations, may hinder relaxation of the heme toward a deoxy state where the doming is toward the proximal histidine (*6*). Time-resolved resonance Raman studies are presently undertaken to further characterize this important transient state.

For WT FixLH in the presence of NO and CO as ligands, the transient spectra were perturbed to a lesser extent than those of the FixLH−$O_2$ complex (*12*), presumably due to the lack of direct interaction between R220 and these two ligands (*6*). In full-length FixL, binding of NO and CO to the heme also diminishes kinase activity, but far less than $O_2$ (*4*). The finding that replacement of R220 also diminishes the perturbation of the spectrum of the NO- and CO-dissociated state (with the exception of the R220H−CO complex; see below) strongly suggests that this residue is also involved in the transmission of the NO and CO signals.

*Kinetics of Rebinding.* The kinetics of picosecond rebinding of NO to heme proteins are generally nonexponential (*23*) and very sensitive to small changes in the heme environment, as has been deduced from studies on myoglobin mutants (*26*, *27*). The observed variation in the kinetics of NO geminate rebinding in the FixLH mutants and WT is in agreement with this notion. All three studied mutant proteins (R220H, -Q, and -A) exhibit slower overall rebinding kinetics than WT. In particular, R220A shows relatively slow rebinding kinetics on the time scale of tens and hundreds of picoseconds. In view of the marked difference in the size of alanine and arginine, and considering the fact that R220 does not appear to interact directly with heme-bound NO in the X-ray structure (*6*), this indicates that the efficient rebinding kinetics in the WT heme domain are due to volume reduction of the distal heme pocket by R220. The same order of efficiency of NO rebinding in the three mutants (histidine > glutamine > alanine) is observed for CO and $O_2$ and correlates as well with a decrease in residue size, suggesting that the volume of the heme pocket plays an important role in the kinetics of rebinding of these ligands.

In WT and the R220Q, -A, -E, and -I mutants, rebinding of CO to the heme does not occur on the time scale up to 4 ns, as is the case in most studied heme proteins. The R220H mutant provides a remarkable exception. In this case, at least ∼60% of dissociated CO decays in a multiexponential way (Figure 1), and the spectra associated with these decay phases differ from those associated with the long-lived state and the steady-state difference spectrum. Resonance Raman experiments have shown the presence of two fractions of the R220H−CO complex, one in an "open" configuration [like CO-bound myoglobin at acidic pH (*28*)] where CO does not interact and one in a "closed" configuration where CO does significantly interact with the protein surroundings, possibly via a CO−histidine hydrogen bond (*16*). The observed pH dependence of the geminate rebinding yield (Figure 1) and its correlation with the pH dependence of the CO stretching frequency (see the Supporting Information) imply that the fraction of R220H that rapidly rebinds CO after dissociation corresponds to the closed configuration, where environmental constraints keep dissociated CO in a favorable position for rebinding. Similar constraints may also explain the unusual 600 ps phase of recombination of $O_2$ to R220H, in view of the hydrogen bond between histidine 220 and the terminal oxygen atom in the R220H oxy complex (*16*).

Using vibrational spectroscopy, as for the R220H−CO complex, two configurations were observed for the R220Q−CO complex, although with a lower population of the closed configuration (*16*). Our finding that in the R220Q mutant no rebinding is observed on the picosecond time scale suggests that in this case the constraints on the dissociated CO either are released rapidly after dissociation or force CO to move away from a favorable rebinding position.

The interaction of the heme with $O_2$ is most relevant for the physiological functioning of the sensor. In WT and all mutants, a decay phase of ∼5−8 ps and a constant phase were observed after excitation; with the exception of R220H (see above), no $O_2$ rebinding occurs on the time scale of 8 ps to 4 ns. Thus, in ∼5 ps, $O_2$ either rebinds or moves to a position much less favorable for rebinding. As similarly a rebinding phase of ∼5 ps is observed for oxyhemoglobin (*25*) and oxymyoglobin (*12*, *29*−*31*), this time constant may correspond to barrierless heme−$O_2$ binding.

The relative amplitude of the constant (>10 ps) phase, only ∼0.1 in WT, is strongly increased in the mutants and practically unity in the R220A mutant. Thus, the very low yield of dissociated oxygen at times of >10 ps is strongly correlated with the presence of arginine at position 220. Our MD simulations indicate indeed that in the mutants $O_2$ can move away rapidly from its position occupied immediately after the Fe−$O_2$ bond is broken. This is particularly clear for the R220A mutant, which has the lowest rebinding yield, but also for the R220I mutant, where steric differences are much smaller.

Our results indicate that the rapid re-formation of the heme−$O_2$ complex as well as the perturbed heme spectrum of the precursor of this state are largely due to the presence of R220 in WT FixLH. These findings are corroborated by the MD simulations of the WT complex that indicate that $O_2$ is mostly kept very close to the heme due to the hydrogen bond between R220 and one of the oxygen atoms.

In a few of the simulations in which $O_2$ does move out of the heme pocket, R220 remains hydrogen bonded with $O_2$ and also sweeps away from the heme (Figure 8). This suggests a correlated movement of R220 and $O_2$. Altogether, prior to ligand dissociation, the H-bond with $O_2$ stabilizes R220 in its conformation toward the heme pocket. After dissociation, R220 can act both as an oxygen trap, allowing fast oxygen recombination, and as a signal "transducer" in case oxygen escapes from the heme pocket. Although the R220 sweep was not observed in all our simulations (limited to 50 ps) where oxygen escapes from the pocket, this charged residue is not likely to be maintained long in the hydrophobic heme environment in the absence of the stabilizing interaction with $O_2$. Indeed, the strain on the heme appears mostly released after the ∼5 ps decay phase (∼90% of dissociated $O_2$), as the spectrum of the weak long-lived spectrum is rather similar to the steady-state difference spectrum (Figure 4). Altogether, these findings strongly suggest that, after of the heme−$O_2$ bond is broken, rebinding with the heme in ∼5

ps competes with oxygen release from the heme pocket on the ~50 ps time scale, the second step in the signaling process, and that the latter process is followed by a marked conformational change of R220, at least in part also on the picosecond time scale. As pointed out in Results, the next step toward the steady-state deoxy structure, a change in the interaction partner of heme propionate 7, is likely to take place on a longer time scale.

## CONCLUDING REMARKS

We have shown that in *Bj*FixL R220 plays an important, though not exclusive, role in exerting strain on the heme after dissociation of the ligand and in caging the oxygen ligand. Previously, we have discussed that the heme pocket of FixL acts as a bistable switch, allowing, after thermal (or light-induced) breaking of the heme−$O_2$ bond, the system either to go back to the oxygen-bound form without further rearrangements or (in ~10% of the cases) to continue to induce structural changes eventually leading to an "anoxy" signal (*12*). Our experimental and computational results presented here indicate that R220 acts as the pivoting element of this picosecond switch.

## ACKNOWLEDGMENT

We thank Jean-Louis Martin for stimulating discussions.

## SUPPORTING INFORMATION AVAILABLE

FTIR characterization of the CO stretching frequency in carboxylated R220H FixLH. This material is available free of charge via the Internet at http://pubs.acs.org.

## REFERENCES

1. Gilles-Gonzalez, M. A., Ditta, G. S., and Helinski, D. R. (1991) A haemoprotein with kinase activity encoded by the oxygen sensor of *Rhizobium meliloti*, *Nature 350*, 170−172.
2. Rodgers, K. R., and Lukat-Rodgers, G. S. (2005) Insights into heme-based $O_2$ sensing from structure−function relationships in the FixL proteins, *J. Inorg. Biochem. 99*, 963−977.
3. Gilles-Gonzalez, M.-A., and Gonzalez, G. (2004) Signal transduction by heme-containing PAS-domain proteins, *J. Appl. Physiol. 96*, 774−783.
4. Tuckerman, J. R., Gonzalez, G., Dioum, E. M., and Gilles-Gonzalez, M. A. (2002) Ligand and oxidation-state specific regulation of the heme-based oxygen sensor FixL from *Sinorhizobium meliloti*, *Biochemistry 41*, 6170−6177.
5. Gong, W., Hao, B., Mansy, S. S., Gonzalez, G., Gilles-Gonzalez, M.-A., and Chan, M. K. (1998) Structure of a biological oxygen sensor: A new mechanism for heme-driven signal transduction, *Proc. Natl. Acad. Sci. U.S.A. 95*, 15177−15182.
6. Gong, W., Hao, B., and Chan, M. K. (2000) New mechanistic insights from structural studies of the oxygen-sensing domain of *Bradyrhizobium japonicum* FixL, *Biochemistry 39*, 3955−3962.
7. Hao, B., Isaza, C., Arndt, J., Soltis, M., and Chan, M. K. (2002) Structure-based mechanism of $O_2$ sensing and ligand discrimination by the FixL heme domain of *Bradyrhizobium japonicum*, *Biochemistry 41*, 12952−12958.
8. Key, J., and Moffat, K. (2005) Crystal Structures of Deoxy and CO-Bound bjFixLH Reveal Details of Ligand Recognition and Signaling, *Biochemistry 44*, 4627−4635.
9. Miyatake, H., Mukai, M., Park, S. Y., Adachi, S. I., Tamura, S., Nakamura, H., Nakamura, K., Tsuchiya, T., Iizuka, T., and Shiro, Y. (2000) Sensory mechanism of oxygen sensor FixL from *Rhizobium meliloti*: Crystallographic, mutagenesis and resonance Raman spectroscopic studies, *J. Mol. Biol. 301*, 415−431.
10. Gilles-Gonzalez, M.-A., Gonzalez, G., Perutz, M., Kiger, L., Marden, M. C., and Poyart, C. (1994) Heme-based sensors, exemplified by the kinase FixL, are a new class of heme protein with distinctive ligand binding and autoxidation, *Biochemistry 33*, 8067−8073.
11. Rodgers, K. R., Lukat-Rodgers, G. S., and Tang, L. (1999) Spectroscopic observation of a FixL switching intermediate, *J. Am. Chem. Soc. 121*, 11241−11242.
12. Liebl, U., Bouzhir-Sima, L., Negrerie, M., Martin, J.-L., and Vos, M. H. (2002) Ultrafast ligand rebinding in the heme domain of the oxygen sensor FixL and Dos: General regulatory implications for heme-based sensors, *Proc. Natl. Acad. Sci. U.S.A. 99*, 12771−12776.
13. Miksovska, J., Suquet, C., Satterlee, J. D., and Larsen, R. W. (2005) Characterization of conformational changes coupled to ligand photodissociation from the heme binding domain of FixL, *Biochemistry 44*, 10028−10036.
14. Park, H., Suguet, C., Satterlee, J. D., and Kang, C. (2004) Insights into Signal Transduction Involving PAS Domain Oxygen-Sensing Heme Proteins from the X-ray Crystal Structure of *Escherichia coli* Dos Heme Domain (Ec DosH), *Biochemistry 43*, 2738−2746.
15. Dunham, C. M., Dioum, E. M., Tuckerman, J. R., Gonzalez, G., Scott, W. G., and Gilles-Gonzalez, M.-A. (2003) A Distal Arginine in Oxygen-Sensing Heme-PAS Domains Is Essential to Ligand Binding, Signal Transduction, and Structure, *Biochemistry 42*, 7701−7708.
16. Balland, V., Bouzhir-Sima, L., Kiger, L., Marden, M. C., Vos, M. H., Liebl, U., and Mattioli, T. A. (2005) Role of Arginine 220 in the Oxygen Sensor FixL from *Bradyrhizobium japonicum*, *J. Biol. Chem. 280*, 15279−15288.
17. Balland, V., Bouzhir-Sima, L., Anxolabéhère-Mallart, E., Boussac, A., Vos, M. H., Liebl, U., and Mattioli, T. A. (2006) Functional implications of the propionate 7−arginine 220 interaction in the FixLH oxygen sensor from *Bradyrhizobium japonicum*, *Biochemistry 45*, 2072−2084.
18. Martin, J.-L., and Vos, M. H. (1994) Femtosecond spectroscopy of ligand rebinding in heme proteins, *Methods Enzymol. 232*, 416−430.
19. Provencher, S. W., and Vogel, R. H. (1983) in *Progress in Scientific Computing* (Deuflhard, P., Ed.) pp 304−319, Birkhauser, Boston.
20. Morgan, J. E., Verkhovsky, M. I., Puustinen, A., and Wikström, M. (1995) Identification of a "Peroxy" Intermediate in Cytochrome $bo_3$ of *Escherichia coli*, *Biochemistry 34*, 15633−15637.
21. Brooks, B. R., Bruccoleri, R. E., Olafson, B. D., Swaminathan, S., and Karplus, M. (1983) CHARMM: A Program for Macromolecular Energy, Minimization, and Dynamics Calculations, *J. Comput. Chem. 4*, 187−212.
22. Lambry, J.-C. (1997) Ph.D. Thesis, University of Orsay, Orsay, France.
23. Vos, M. H., and Martin, J.-L. (1999) Femtosecond processes in proteins, *Biochim. Biophys. Acta 1411*, 1−20.
24. Borisov, V. B., Liebl, U., Rappaport, F., Martin, J.-L., Zhang, J., Gennis, R. B., Konstantinov, A. A., and Vos, M. H. (2002) Interactions between heme *d* and heme $b_{595}$ in quinol oxidase *bd* from *Escherichia coli*: A photoselection study using femtosecond spectroscopy, *Biochemistry 41*, 1654−1662.
25. Petrich, J. W., Poyart, C., and Martin, J.-L. (1988) Photophysics and reactivity of heme proteins: A femtosecond absorption study of hemoglobin, myoglobin and protoheme, *Biochemistry 27*, 4049−4060.
26. Carlson, M. L., Regan, R., Elber, R., Li, H., Phillips, G. N., Jr., Olson, J. S., and Gibson, Q. H. (1994) Nitric oxide recombination to double mutants of myoglobin: Role of ligand diffusion in a fluctuating heme pocket, *Biochemistry 33*, 10597−10606.
27. Petrich, J. W., Lambry, J.-C., Balasubramanian, S., Lambright, D. G., Boxer, S. G., and Martin, J.-L. (1994) Ultrafast measurements of geminate recombination of NO with site-specific mutants of human myoglobin, *J. Mol. Biol. 238*, 437−444.
28. Ramsden, J., and Spiro, T. G. (1989) Resonance Raman evidence that distal histidine protonation removes the steric hindrance to upright binding of carbon monoxide by myoglobin, *Biochemistry 28*, 3125−3128.

29. Walda, K. N., Liu, X. Y., Sharma, V. S., and Magde, D. (1994) Geminate recombination of diatomic ligands CO, $O_2$, and NO with myoglobin, *Biochemistry 33*, 2198−2209.
30. Ye, X., Demidov, A., and Champion, P. M. (2002) Measurements of the Photodissociation Quantum Yields of MbNO and $MbO_2$ and the Vibrational Relaxation of the Six-Coordinate Heme Species, *J. Am. Chem. Soc. 124*, 5914−5924.
31. Wang, Y., Baskin, J. S., Xia, T., and Zewail, A. H. (2004) Human myoglobin recognition of oxygen: Dynamics of the energy landscape, *Proc. Natl. Acad. Sci. U.S.A. 101*, 18000−18005.
32. Sayle, R. A., and Milner-White, E. J. (1995) RASMOL: Biomolecular graphics for all, *Trends Biochem. Sci. 20*, 374−376.

BI060012I